Journal of
Materials Chemistry C

Accepted Manuscript

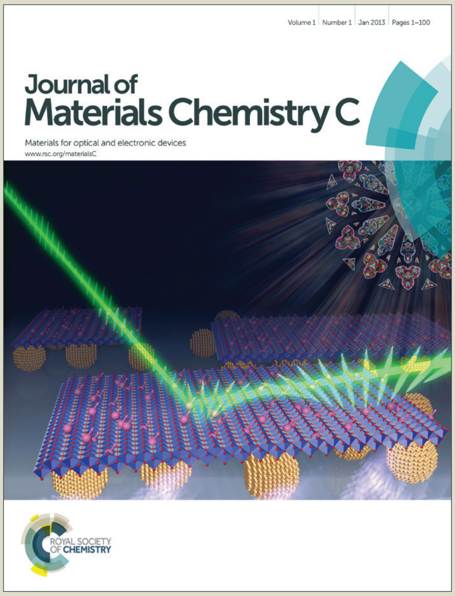

ROYAL SOCIETY
OF CHEMISTRY

www.rsc.org/materialsC

Journal of Materials Chemistry C RSCPublishing

COMMUNICATION

Cite this: DOI: 10.1039/x0xx00000x

Received 00th January 2012,
Accepted 00th January 2012

DOI: 10.1039/x0xx00000x

www.rsc.org/

Small Band Gap Polymers Incorporating a Strong Acceptor, Thieno[3,2-*b*]thiophene-2,5-dione, with P-Channel and Ambipolar Charge Transport Characteristics

Itaru Osaka,[a,b,c,]* Toru Abe,[a] Hiroki Mori,[a] Masahiko Saito,[a] Noriko Takemura,[b] Tomoyuki Koganezawa,[d] and Kazuo Takimiya[a,b,]*

We present new donor–acceptor semiconducting polymers based on a strong acceptor unit, thieno[3,2-*b*]thiophene-2,5-dione (TTD). The polymers afford a deep LUMO energy level of around –4 eV while preserving a relatively low-lying HOMO energy level of below –5 eV and a quite small optical band gap of 1.2 eV. Interestingly, bottom-gate-top-contact transistor devices based on the polymers demonstrate p-channel behavior with high hole-mobilites of 1.38 cm^2 V^{-1} s^{-1}, whereas top-gate-bottom-contact devices show ambipolar behavior with hole and electron mobilities of ~0.12 and ~0.20 cm^2 V^{-1} s^{-1}, respectively. These results indicate great promise of TTD as the building unit for high-performance semiconducting polymers.

Semiconducting polymers with "donor (D)–acceptor (A)" motifs (D-A polymers), where electron rich (donor) and electron poor (acceptor) units are copolymerized, has recently been the focus of attention in organic electronics.[1] Their use as active layer materials have brought about significant advances in organic field-effect transistors (OFETs)[2] and organic photovoltaics (OPVs).[3] In particular, high charge carrier mobilities surpassing 1 cm^2 V^{-1} s^{-1} in both n-channel/ambipolar[4a,5,6] and p-channel OFETs[7,8,9] based on D-A polymers have been reported, which have motivated synthetic chemists/materials scientists to explore further high performance semiconducting polymers.

Of our particular interest, as well as of importance in the development of new materials, is to explore A units that possess strong electron affinity and ensure coplanarity of the polymer backbone. The use of such A units, e.g. naphthalenedicarboximide (NDI),[4] diketopyrrolopyrrole (DPP),[5,6a,8] and isoindigo,[9] in D-A polymers significantly reduces LUMO energy levels (E_{LUMO}) while they possess relatively deep HOMO energy levels (E_{HOMO}), since the energy levels of D-A polymers are resulted from the orbital mixing of the D and A units. The deep E_{LUMO} is crucial for the n-channel/ambipolar characteristics. D-A polymers with such A units could also give rise to strong intermolecular π–π interactions and thus to highly organized polymer chains in the solid state, which facilitates the charge transport property.[4b,7,8a,9,10] Hence, regardless of the charge carrier polarity, the exploration of new strong A units is highly important for the development of high performance semiconducting polymers.

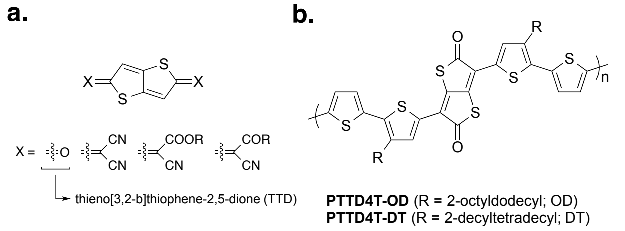

Figure 1. (a) Chemical structures of thienothiophene-based quinoidal compounds. (b) Chemical structure of thienothiophenedione (TTD)-based polymers synthesized in this work (PTTD4Ts).

We here propose thieno[3,2-*b*]thiophene-2,5-dione (TTD; Figure 1a)[11] as a new A unit for semiconducting polymers, which have been of great interest to us since our work on the series of thienoquinoid small molecular semiconductors (Figure 1a).[12] With two ketones at the α-position of quinoidal thieno[3,2-*b*]thiophene, TTD possesses strong electron accepting nature. Recently, such quinoidal cores have been also introduced in semiconducting polymers.[13] Although TTD is not an aromatic heterocycle, when thiophenes are linked at the β-position of TTD, the resulting unit allows a fully π-conjugated structure along with high coplanarity,[14] where TTD can be viewed as a *trans*-butadiene moiety that is bridged to form thiolactones (Figure 1b). In this paper, we report the synthesis, electronic properties, and thin-film structures of TTD-based semiconducting polymers (Figure 1b), and their use in OFETs.

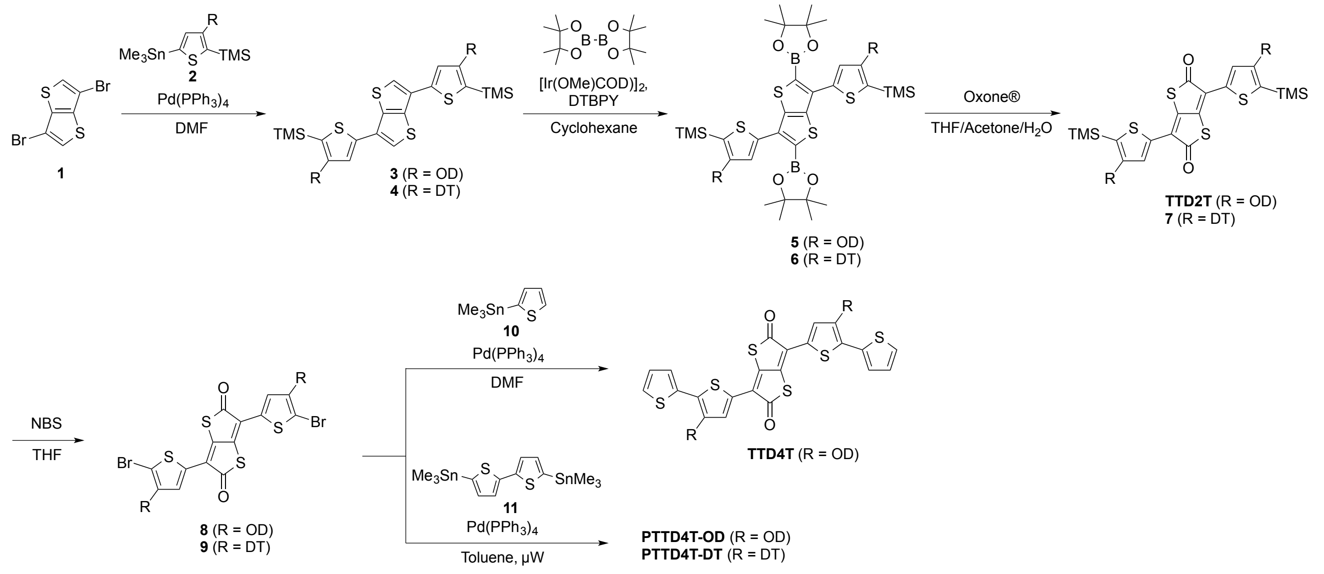

Scheme 1. Synthetic route to the TTD-based polymers and model compounds.

Scheme 1 shows the synthesis of the TTD-based copolymers, PTTD4Ts, where a simple quaterthiophene unit is used as the D unit for better understanding the nature of TTD when incorporated into the polymer backbone. 2-Octyldodecyl (OD) and 2-decyltetradecyl (DT) branched alkyl groups are chosen as the side chain to give the polymers sufficient solubility and processability. 3,6-Dibromothieno[3,2-*b*]thiophene (**1**) was first cross-coupled with 2-trimethylsilyl-5-trimethylstannyl-3-alkylthiophene (**2**) to afford **3** (R = OD) and **4** (R = DT), which were then directly borylated with pinacol diborane in the presence of a Ir catalyst, yielding **5** and **6**, respectively.[15] **5** and **6** were oxidized with potassium peroxysulfate (Oxone®) to form TTD derivatives (**TTD2T** for R = OD, and **7** for R = DT), which were subsequently brominated at the α-position of the alkylthiophene moiety to give **8** and **9**, respectively. **8**, with R = OD, was cross-coupled with stannylated thiophene (**10**) to give **TTD4T**, the repeat unit for the polymer. Finally, **8** and **9** were copolymerized with distannylated bithiophene (**11**) via the Stille coupling reaction to afford PTTD4T-OD and -DT, respectively. PTTD4T-OD and -DT are soluble in chlorobenzene (CB) or *o*-dichlorobenzene (DCB) at above 120 ºC and at around 60 ºC, respectively. The number average molecular weight (M_n) of the polymers was higher than 30 kDa with the polydispersity index (PDI) of around 2.0 (Table 1).

Cyclic voltammetry in the solution was carried out for TTD2T, TTD4T, and PTTD4T-OD, in which, for PTTD4T-OD, the low molecular weight sample (M_n = 4300) obtained as the minor fraction collected with chloroform at the time of Soxhlet extraction was used (Figure 2a). From the redox onset potential, E_{LUMO} and E_{HOMO} of TTD2T are estimated to be –3.8 and –5.9 eV, respectively, evidencing that the TTD moiety indeed possesses strong electron accepting nature. Notably, E_{LUMO} of –3.8 eV for TTD2T was comparable to that for the model compound of an NDI-based polymers, –3.8 eV (Figure S1), superior n-channel/ambipolar semiconductor. It should also be noted that while E_{LUMO} for TTD4T and PTTD4T-OD are both similar to that for TTD2T, –3.8 eV, E_{HOMO} gradually elevates from –5.9 eV (TTD2T) to –5.5 and –5.1 eV, respectively, indicating that the significantly reduced band gap of PTTD4T, compared to TTD4T, was brought about by the rise of E_{HOMO} (Figure 2c). This could be explained by the geometry of molecular orbitals of TTD2T and TTD4T calculated with the DFT method at the B3LYP-6-31 g(d) level; the HOMO coefficient is fully distributed over the structure, whereas the LUMO is relatively

Table 1. Polymer properties.

Side chain	M_n (kDa) [a]	M_w (kDa) [a]	PDI [a]	E_{HOMO} (eV) [b]	E_{LUMO} (eV) [c]	E_g (eV) [d]	λ_{max} (nm) [e]		μ_{BGTC} (cm^2 V^{-1} s^{-1}) [f]	μ_{TGBC} (cm^2 V^{-1} s^{-1}) [g]	
							solution	film		hole	electron
OD	34.2	62.3	1.8	–5.3 (–5.1)	–4.1 (–3.8)	1.2	835	830	0.39	0.034	0.13
DT	33.0	59.0	1.8	–5.3	–4.1	1.2	818	828	1.38	0.12	0.20

[a] Determined by GPC using polystyrene standard and DCB as the eluent at 140 °C. [b] HOMO energy levels determined by photoelectron spectroscopy in air (PESA). In the parenthesis is the value estimated by cyclic voltammetry using the low molecular weight sample. [c] LUMO energy levels estimated by adding the band gap (E_g) to E_{HOMO} obtained from PESA. In the parenthesis is the value determined by cyclic voltammetry. [d] Band gaps estimated from the absorption onset. [e] Absorption maxima in the solution and film. [f] Maximum hole mobilities evaluated by bottom-gate top-contact (BGTC) OFET devices. [g] Maximum hole and electron mobilities evaluated by top-gate bottom-contact (TGBC) OFET devices.

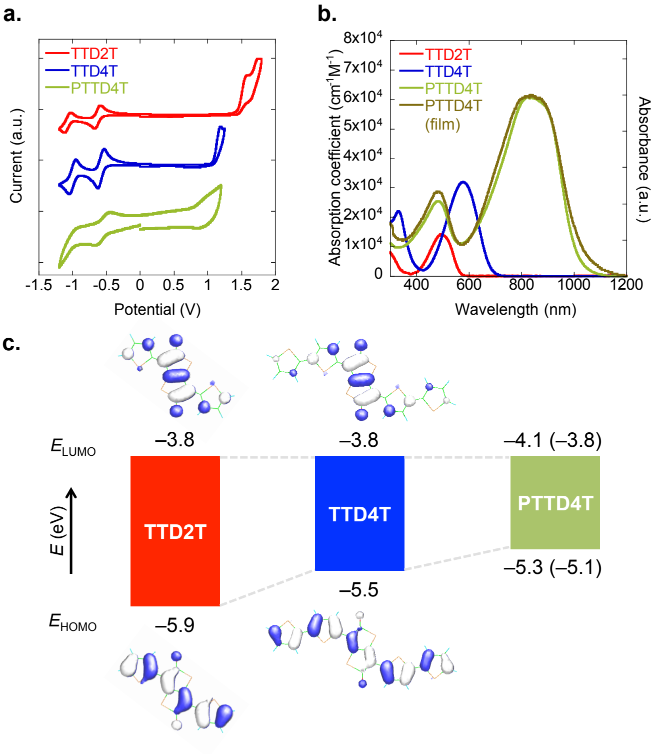

Figure 2. (a) Cyclic voltammograms and (b) UV-vis absorption spectra of TTD2T, TTD4T, and PTTD4T (R = OD for all the compounds). Cyclic voltammetry was carried out in the DCM solution. Absorption spectra were measured using the DCB solution and the film for PTTD4T-OD. (c) HOMO and LUMO energy levels (E_{HOMO} and E_{LUMO}) and HOMO and LUMO geometry calculated by the DFT method at the B3LYP/6-31(d) level for TTD2T, TTD4T, and PTTD4T. E_{HOMO} and E_{LUMO} for TTD2T and TTD4T were evaluated by CV. E_{HOMO} for PTTD4T was determined by PESA, and E_{LUMO} was determined by the addition of E_g. In the parenthesis are the values evalutated by CV using the low molecular weigth sample.

localized on the TTD unit (Figure 2c). The HOMO delocalization in this system is in fact far prominent as compared to other typical D–A polymer systems.[16] Photoelectron spectroscopy in air (PESA) was also carried out with the polymer thin film, which gave E_{HOMO} of –5.3 eV regardless of the side chain length (Table 1). E_{LUMO} estimated by subtracting the optically determined E_g (vida infra) from E_{HOMO} estimated by PESA is –4.1 eV.

UV-vis absorption spectra of TTD2T, TTD4T, and PTTD4T-OD in the dilute solution are depicted in Figure 2b. TTD2T already had an absorption maximum (λ_{max}) at relatively long wavelength region, 493 nm, implying the presence of D–A interaction. TTD4T showed bathochromic shift of λ_{max} to 577 nm, reflecting the π-extension by attaching two thiophenes, along with the twice increased absorption coefficient (ε) of 3.2×10^4 $\mathrm{cm^{-1}\ M^{-1}}$. It is interesting to note that λ_{max} of PTTD4T-OD significantly red-shifted to 835 nm, with further increased ε of 6.1×10^4 $\mathrm{cm^{-1}\ M^{-1}}$, compared to TTD4T, and the absorption onset reaches near-IR region of 1030 nm, which corresponds to E_g of 1.20 eV. This marked red-shift in the absorption spectra from the repeat unit to the polymer means that the polymer backbone possesses a quite effectively developed π-conjugation, which is fairly unique compared to the other D–A polymers.[17] The significantly elongated effective π-conjugation length originates in the elevation of E_{HOMO} as described

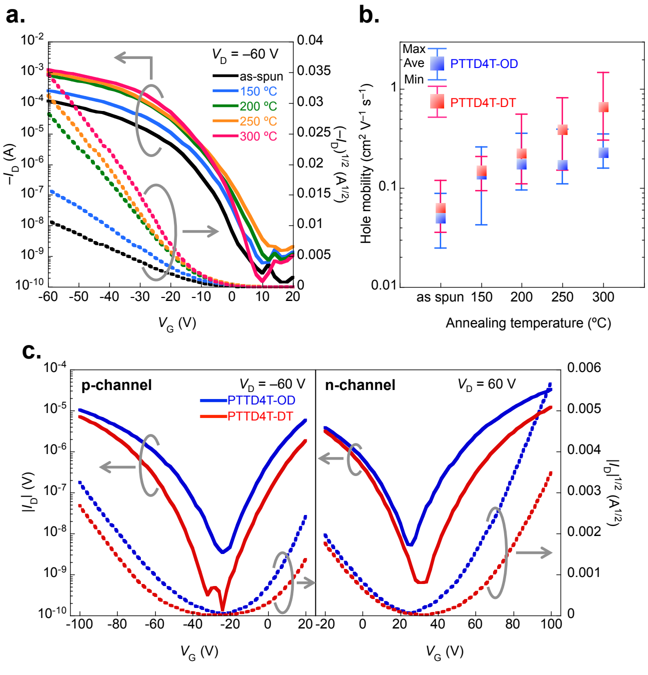

Figure 3. (a) Typical transfer characteristics of OFETs based on PTTD4T-DT with the BGTC configuration. (b) Hole mobilities evaluated from BGTC devices as a function of annealing temperature. (c) Typical transfer characteristics of PTTD4T-based TGBC devices.

above. Absorption spectrum of PTTD4T-DT was mostly identical to PTTD4T-OD (Figure S3), and PTTD4Ts in the thin film gave slightly broadened spectra compared to those in the solution (Figure 2b).

Polymer OFETs were tested with the bottom-gate top-contact (BGTC) and top-gate bottom-contact (TGBC) configurations. In the BGTC device, polymer films were fabricated on the Si/SiO$_2$ substrate treated with 1*H*,1*H*,2*H*,2*H*-perfluorodecyltriethoxysilane (FDTS), which enhances charge accumulation and crystallinity.[18] PTTD4Ts gave only p-channel behavior (Figure 3a), though they possess E_{LUMO} of around –4 eV that is supposed to be a borderline for the ambient n-channel operation.[19] On the other hand, interestingly, in the TGBC devices PTTD4Ts showed ambipolar characteristics, possibly as a result of the passivation by the gate insulator on top of the polymer layer, preventing the electron trapping by atmospheric moisture. The hole-mobilities of PTTD4Ts determined from the BGTC device were moderately high, around 0.2–0.3 $\mathrm{cm^2\ V^{-1}\ s^{-1}}$, when annealed at 150 ºC (Figure 3a, b). PTTD4T-OD, when annealed at higher temperatures, exhibited slightly higher mobilities up to 0.39 $\mathrm{cm^2\ V^{-1}\ s^{-1}}$. On the contrary, PTTD4T-DT shows gradual increase in the mobility at higher annealing temperatures, and it reached 1.38 $\mathrm{cm^2\ V^{-1}\ s^{-1}}$, with the average of 0.66 $\mathrm{cm^2\ V^{-1}\ s^{-1}}$, when annealed at 300 ºC (Figure 3a, b). The on/off ratios are typically 10^5–10^7. All the transistor parameters are summarized in Table S1. Figure 3c shows the typical transfer curves of the TGBC devices, in which PTTD4T-OD and -DT were annealed at 200 and 300 ºC, respectively. The hole- and electron-mobilities were estimated to be 0.034 and 0.13 $\mathrm{cm^2\ V^{-1}\ s^{-1}}$ for PTTD4T-OD, and 0.12 and 0.20 $\mathrm{cm^2\ V^{-1}\ s^{-1}}$ for PTTD4T-DT, respectively.

To correlate these high semiconducting characteristics of the polymers with their microstructure, two-dimensional grazing incidence

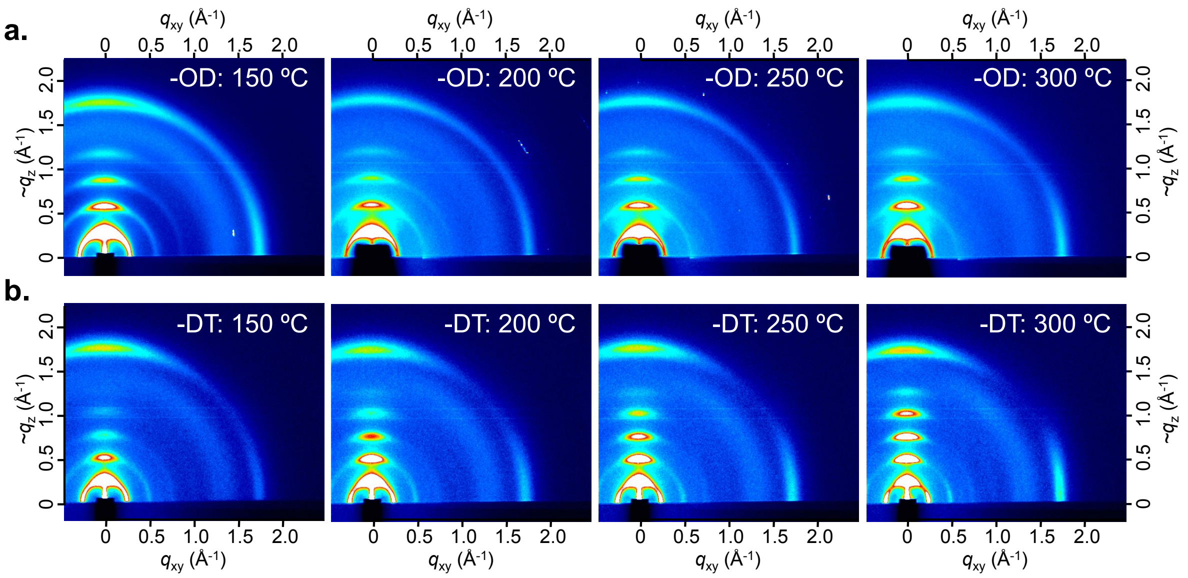

Figure 4. 2D-GIXD images of the PTTD4T-OD (a) and -DT (b) thin films annealed at 150, 200, 250, and 300 ºC, respectively.

X-ray diffraction (2D-GIXD) measurements were performed (Figure 4). The PTTD4T-OD film annealed at 150 °C afforded diffractions corresponding to the lamellar structure up to the forth order along the q_z axis (Figure 4a), indicating the well-ordered lamellar structure in the crystalline domain.[20] However, the crystallites oriented randomly against the surface normal, as evident from that lamellar (q = 0.30 Å^{-1}) and π–π stacking (q = 1.73 Å^{-1}) diffractions appeared as arc and ring, respectively. Nevertheless, the π–π stacking distance (d_π) was estimated to be 3.63 Å, which was relatively narrow for the semiconducting polymers, most probably as a result of the highly coplanar structure and strong intermolecular interaction of the PTTD4T backbone. In addition, almost the same diffraction pattern was observed in the thin films annealed at different temperatures, being consistent with the mobility trend. In the PTTD4T-DT film (Figure 4b) annealed at 150 °C, on the other hand, the π–π stacking diffraction was more pronounced in the q_z axis compared to the q_{xy} axis (d_π = 3.63 Å), suggesting that PTTD4T-DT formed face-on crystallites to larger extent than PTTD4T-OD. It is interesting to note that the annealing the PTTD4T-DT film at higher temperatures gradually increased the population of edge-on crystallites (Table S2). Furthermore, the crystallinity apparently increases at higher annealing temperatures, as the coherence length of the crystallite, calculated by the Scherrer equation using the lamellar peaks, became larger (Table S3).[21] These changes in the structural order as a function of the annealing temperature agree well with the mobility trend. The distinct behavior between PTTD4T-OD and -DT could be attributed to the different molecular flexibility, where the polymer with the longer side chain (DT) is more flexible, enabling the rearrangement of the packing structure. This also implies that the PTTD4T backbone is quite rigid and has strong intermolecular interactions.

Although recently extraordinarily high mobilities of ~10 cm^2 V^{-1} s^{-1}, in particular for DPP-based polymers, have been reported, the observed mobilities of around 1 cm^2 V^{-1} s^{-1} in PTTD4Ts are still high for semiconducting polymers. However, the microstructure in the thin film, namely, the π–π stacking structure with an edge-on motif (face-on crystallites are also present) is quite common and d_π of ca. 3.6 Å is not too narrow, which may not fully rationalize their semiconducting performances. We speculate that these high mobilities for PTTD4Ts, despite the quite familiar structural features, might be, in part, attributed to the significantly developed backbone π-conjugation, in which HOMO is highly delocalized, as evident from the computation and the electrochemical and optical measurements. This delocalization would facilitate both the intramolecular and intermolecular electronic coupling and thus charge transport.[8a,22] In addition, the possibly high intramolecular charge transport may compensate the in-plane charge transport in the face-on crystallite that is thought to be detriment for the transistor configuration. Thus, combined with the crystalline π–π stacking structure, the highly developed π-conjugation may offer well-established in-plane 2D (intra- and inter-chain) electronic structures. This should be beneficial for the efficient charge transport in polycrystalline films, in which the polymer crystallites are isotropic within the substrate plane, as has been discussed in small molecular semiconductors that the herringbone-packed molecule with the 2D electronic structure is advantageous for high mobilities over the π-stacked molecule with 1D electronic structure.[22]

Conclusions

In conclusion, we have presented new semiconducting polymers with a strong acceptor unit, TTD. The polymers were found to have deep E_{LUMO} while preserving relatively deep E_{HOMO}, along with a quite small E_g as well as highly developed π-conjugation. The polymers exhibited hole mobilities as high as 1.38 cm^2 V^{-1} s^{-1} in BGTC-OFETs and ambipolar characteristics with hole and electron mobilities of 0.12 and 0.20 cm^2 V^{-1} s^{-1} in TGBC-OFETs. With the quite unique electronic structure and attractive electrical features, TTD is indeed a fascinating acceptor unit for the development of high-performance semiconducting polymers.

Notes and references

[a] Emergent Molecular Function Research Group, RIKEN Center for Emergent Matter Science (CEMS), 2-1 Hirosawa, Wako, Saitama 351-0198 (Japan). itaru.osaka@riken.jp, takimiya@riken.jp

[b] Department of Applied Chemistry, Graduate School of Engineering, Hiroshima University, 1-4-1 Kagamiyama, Higashi-Hiroshima, Hiroshima, 739-8527 (Japan).

[c] Precursory Research for Embryonic Science and Technology, Japan Science and Technology Agency, Chiyoda-ku, Tokyo 102-0075 (Japan).

[d] Japan Synchrotron Radiation Research Institute, 1-1-1 Kouto, Sayo-cho, Sayo-gun, Hyogo 679-5198 (Japan).

† Electronic Supplementary Information (ESI) available: [Details of synthesis, instrumentation, device fabrication and measurements, crystal structure of the model compound, polymer properties, device characteristics, and film structures and morphologies]. See DOI: 10.1039/c000000x/

1 (a) A. Facchetti, *Chem. Mater.* 2011, **23**, 733–758. (b) P. M. Beaujuge, J. M. J. Fréchet, *J. Am. Chem. Soc.* 2011, **133**, 20009–20029.

2 (a) M. Zhang, H. N. Tsao, W. Pisula, C. Yang, A. K. Mishra, K. Müllen, *J. Am. Chem. Soc.* 2007, **129**, 3472–3473. (b) I. Osaka, G. Sauvé, R. Zhang, T. Kowalewski, R. D. McCullough, *Adv. Mater.* 2007, **19**, 4160–4165. (c) L. Bürgi, M. Turbiez, R. Pfeiffer, F. Bienewald, H. Kirner, C. Winnewisser, *Adv. Mater.* 2008, **20**, 2217–2224.

3 (a) D. Mühlbacher, M. Scharber, M. Morana, Z. Zhu, D. Waller, R. Gaudiana, C. Brabec, *Adv. Mater.* 2006, **18**, 2884–2889. (b) M. M. Wienk, M. Turbiez, J. Gilot, R. A. J. Janssen, *Adv. Mater.* 2008, **20**, 2556–2560.

4 (a) H. Yan, Z. Chen, Y. Zheng, C. Newman, J. R. Quinn, F. Dötz, M. Kastler, A. Facchetti, *Nature* 2009, **457**, 679–686. (b) J. Rivnay, M. F. Toney, Y. Zheng, I. V. Kauvar, Z. Chen, V. Wagner, A. Facchetti, A. Salleo, *Adv. Mater.* 2010, **22**, 4359–4363.

5 A. J. Kronemeijer, E. Gili, M. Shahid, J. Rivnay, A. Salleo, M. Heeney, H. Sirringhaus, *Adv. Mater.* 2012, **24**, 1558–1565.

6 (a) J. D. Yuen, J. Fan, J. Seifter, B. Lim, R. Hufschmid, A. J. Heeger, F. Wudl, *J. Am. Chem. Soc.* 2011, **133**, 20799–20807. (b) J. Fan, J. D. Yuen, M. Wang, J. Seifter, J. -H. Seo, A. R. Mohebbi, D. Zakhidov, A. J. Heeger, F. Wudl, *Adv. Mater.* 2012, **24**, 2186–2190.

7 (a) H. N. Tsao, D. M. Cho, I. Park, M. R. Hansen, A. Mavrin-skiy, D. Y. Yoon, R. Graf, W. Pisula, H. W. Spiess, K. Müllen, *J. Am. Chem. Soc.* 2011, **133**, 2605–2612. (b) W. Zhang, J. Smith, S. E. Watkins, R. Gysel, M. McGehee, A. Salleo, J. Kirkpatrick, S. Ashraf, T. Anthopoulos, M. Heeney, *J. Am. Chem. Soc.* 2010, **132**, 11437–11439.

8 (a) H. Bronstein, Z. Chen, R. S. Ashraf, W. Zhang, J. Du, J. R. Durrant, P. S. Tuladhar, K. Song, S. E. Watkins, Y. Geerts, M. M. Wienk, R. A. J. Janssen, T. Anthopoulos, H. Sirringhaus, M. Heeney, I. McCulloch, *J. Am. Chem. Soc.* 2011, **133**, 3272–3275. (b) Y. Li, P. Sonar, S. P. Singh, M. S. Soh, M. van Meurs, J. Tan, *J. Am. Chem. Soc.* 2011, **133**, 2198–2204. (c) H. Chen, Y. Guo, G. Yu, Y. Zhao, J. Zhang, D. Gao, H. Liu, and Y. Liu, *Adv. Mater.* 2012, **24**, 4618–4622. (d) J. Li, Y. Zhao, H. S. Tan, Y. Guo, C. Di, G. Yu, Y. Liu, M. Lin, S. H. Lim, Y. Zhou, H. Su, B. S. Ong, *Sci. Rep.* 2012, **2**, 754.

9 (a) J. Mei, D. H. Kim, A. L. Ayzner, M. F. Toney, Z. Bao, *J. Am. Chem. Soc.* 2011, **133**, 20130–20133. (b) T. Lei, J. -H. Dou, J. Pei, *Adv. Mater.* 2012, **24**, 6457–6461. (c) T. Lei, Y. Cao, X. Zhou, Y. Peng, J. Bian, J. Pei, *Chem. Mater.* 2012, **24**, 1762–1770.

10 (a) I. Osaka, M. Shimawaki, H. Mori, I. Doi, E. Miyazaki, T. Koganezawa, K. Takimiya, *J. Am. Chem. Soc.* 2012, **134**, 3498–3507. (b) I. Osaka, T. Abe, M. Shimawaki, T. Koganezawa, K. Takimiya, *ACS Macro Lett.* 2012, **1**, 437–440.

11 S. Chen, A. Bolag, J. Nishida, Y. Yamashita, *Chem. Lett.* 2011, **40**, 998–1000.

12 (a) Y. Suzuki, E. Miyazaki, K. Takimiya, *J. Am. Chem. Soc.* 2010, **132**, 10453–10466. (b) Y. Suzuki, M. Shimawaki, E. Miyazaki, I. Osaka, K. Takimiya, *Chem. Mater.* 2011, **23**, 795–804.

13 (a) W. Cui, J. Yuen, F. Wudl, *Macromolecules* 2011, **44**, 7869–7873. (b) W. Hong, B. Sun, C. Guo, J. Yuen, Y. Li, S. Lu, C. Huang, A. Facchetti, *Chem. Commun*. 2012, **49**, 484–486. (c) I. Welterlich, O. Charov, B. Tieke, *Macromolecules* 2012, **45**, 4511–4519. (d) M. Kirkus, S. Knippenberg, D. Beljonne, J. Cornil, R. A. J. Janssen, S. C. J. Meskers, *J. Phys. Chem. A* 2013, **117**, 2782–2789. (e) S. Lu, M. Drees, Y. Yao, D. Boudinet, H. Yan, H. Pan, J. Wang, Y. Li, H. Usta, A. Facchetti, *Macromolecules* 2013, **46**, 3895–3906.

14 Coplanarity of the TTD–thiophene junction is confirmed by the X-ray analysis of the single crystal of a model compound, TTD2T with R = H (Figure S2).

15 T. Ishiyama, J. Takagi, K. Ishida, N. Miyaura, N. R. Anastasi, J. F. Hartwig, *J. Am. Chem. Soc.* 2002, **124**, 390–391.

16 K. Takimiya, I. Osaka, M. Nakano, *Chem. Mater.* 2013, DOI: 10.1021/cm4021063.

17 As reported on a naphthobisthiadiazole (NTz) polymer in reference 10a, $\Delta\lambda$, shift of $\lambda_{\max}$ from the model compound (NTz2T; bithienyl-NTz) to the corresponding polymer (PNTz4T; poly(quaterthienyl-NTz), was 216 nm, whereas $\Delta\lambda$ in the TTD system was 342 nm even though the $\lambda_{\max}$ of both NTz2T and TTD2T were mostly the same.

18 (a) S. Kobayashi, T. Nishikawa, T. Takenobu, S. Mori, T. Shimoda, T. Mitani, H. Shimotani, N. Yoshimoto, S. Ogawa, Y. Iwasa, *Nat. Mater.* 2004, **3**, 317–322. (b) T. Umeda, D. Kumaki, S. Tokito, *J. Appl. Phys.* 2009, **105**, 024516. (c) K. Nakayama, M. Uno, T. Nishikawa, Y. Nakazawa, J. Takeya, *Org. Electron.* 2010, **11**, 1620–1623. (d) I. Osaka, T. Abe, S. Shinamura, K. Takimiya, *J. Am. Chem. Soc.* 2011, **133**, 6852–6860.

19 (a) D. M. de Leeuw, M. M. J. Simenon, A. R. Brown, R. E. F. Einerhand, *Synth. Met.* 1997, **87**, 53–59. (b) T. D. Anthopoulos, G. C. Anyfantis, G. C. Papavassiliou, D. M. de Leeuw, *Appl. Phys. Lett.* 2007**, 90**, 122105. (c) B. A. Jones, A. Facchetti, M. R. Wasielewski, T. J. Marks, *J. Am. Chem. Soc.* 2007, **129**, 15259–15278.

19 M. L. Chabinyc, M. F. Toney, R. J. Kline, I. McCulloch, M. Heeney, *J. Am. Chem. Soc.* 2007, **129**, 3226–3237.

20 I. Osaka, S. Shinamura, T. Abe, K. Takimiya, *J. Mater. Chem. C* 2013, **1**, 1297–1304.

21 (a) D. M. DeLongchamp, R. J. Kline, Y. Jung, E. K. Lin, D. A. Fischer, D. J. Gundlach, S. K. Cotts, A. J. Moad, L. J. Richter, M. F. Toney, M. Heeney, I. McCulloch, *Macromolecules* 2008, **41**, 5709–5715. (b) J. T. Rogers, K. Schmidt, M. F. Toney, E. J. Kramer, Gu. C. Bazan, *Adv. Mater.* 2011, **23**, 2284–2288. (c) R. J. Roe, Methods of X-ray and Neutron Scattering in Polymer Science, Oxford University Press, New York 2000.

22 (a) J. -L. Brédas, D. Beljonne, V. Coropceanu, J. Cornil, *Chem. Rev.* 2004, **104**, 4971–5004. (b) K. Takimiya, S. Shinamura, I. Osaka, E. Miyazaki, *Adv. Mater.* 2011, **23**, 4347–4370.

TOC entry.

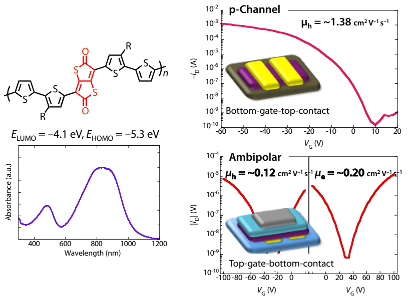

text.

Novel small band gap semiconducting polymers incorporating thienothiophenedione exhibited high hole mobilities of ~1.38 cm^2 V^{-1} s^{-1}.